Title

Eri1 regulates microRNA homeostasis and mouse lymphocyte development and antiviral function

Journal

Blood, 120(1)

ISSN

0006-4971

Authors

Thomas, Molly F
Abdul-Wajid, Sarah
Panduro, Marisella
et al.

Publication Date

2012-07-05

DOI

10.1182/blood-2011-11-394072

Peer reviewed

blood

2012 120: 130-142
Prepublished online May 21, 2012;
doi:10.1182/blood-2011-11-394072

Eri1 regulates microRNA homeostasis and mouse lymphocyte development and antiviral function

Molly F. Thomas, Sarah Abdul-Wajid, Marisella Panduro, Joshua E. Babiarz, Misha Rajaram, Prescott Woodruff, Lewis L. Lanier, Vigo Heissmeyer and K. Mark Ansel

Blood (print ISSN 0006-4971, online ISSN 1528-0020), is published weekly by the American Society of Hematology, 2021 L St, NW, Suite 900, Washington DC 20036.

Eri1 regulates microRNA homeostasis and mouse lymphocyte development and antiviral function

Molly F. Thomas,[1,2] Sarah Abdul-Wajid,[1,2] Marisella Panduro,[1,2] Joshua E. Babiarz,[3] Misha Rajaram,[4] Prescott Woodruff,[4,5] Lewis L. Lanier,[1] Vigo Heissmeyer,[6] and K. Mark Ansel[1,2]

[1]Department of Microbiology and Immunology, University of California, San Francisco, San Francisco, CA; [2]Sandler Asthma Basic Research Center, University of California, San Francisco, San Francisco, CA; [3]Eli and Edythe Broad Center of Regeneration Medicine and Stem Cell Research, Center for Reproductive Sciences, and Department of Urology, University of California, San Francisco, San Francisco, CA; [4]Cardiovascular Research Institute, University of California, San Francisco, San Francisco, CA; [5]Division of Pulmonary and Critical Care Medicine, Department of Medicine, University of California, San Francisco, San Francisco, CA; and [6]Helmholtz Zentrum München, German Research Center for Environmental Health, Institute of Molecular Immunology, Munich, Germany

Natural killer (NK) cells play a critical role in early host defense to infected and transformed cells. Here, we show that mice deficient in Eri1, a conserved 3′-to-5′ exoribonuclease that represses RNA interference, have a cell-intrinsic defect in NK-cell development and maturation. *Eri1*$^{-/-}$ NK cells displayed delayed acquisition of Ly49 receptors in the bone marrow (BM) and a selective reduction in Ly49D and Ly49H activating receptors in the periphery. Eri1 was required for immune-mediated control of mouse CMV (MCMV) infection. Ly49H^{+} NK cells deficient in Eri1 failed to expand efficiently during MCMV infection, and virus-specific responses were also diminished among *Eri1*$^{-/-}$ T cells. We identified miRNAs as the major endogenous small RNA target of Eri1 in mouse lymphocytes. Both NK and T cells deficient in Eri1 displayed a global, sequence-independent increase in miRNA abundance. Ectopic Eri1 expression rescued defective miRNA expression in mature *Eri1*$^{-/-}$ T cells. Thus, mouse Eri1 regulates miRNA homeostasis in lymphocytes and is required for normal NK-cell development and antiviral immunity. (*Blood*. 2012;120(1):130-142)

Introduction

Natural killer (NK) cells are important lymphocyte effectors that participate in early immune responses against tumors and pathogen-infected cells by secreting cytokines and directly lysing target cells.[1] Unlike T and B cells, which become activated through single antigen-specific receptors, NK-cell activation is controlled by the integration of signals from activating and inhibitory receptors.[2] The inhibitory mouse Ly49 receptors are a highly polymorphic class of molecules that predominantly recognize MHC class I ligands. In contrast, Ly49 activating receptors can bind MHC class I molecules or ligands expressed on transformed or infected cells. For example, Ly49H recognizes the m157 glycoprotein encoded by mouse CMV (MCMV).[3,4] During NK-cell development in the bone marrow (BM), Ly49 receptors are acquired in a stochastic fashion just before cells undergo a major proliferative burst and are released into the periphery. Humans and mice with selective NK-cell deficiencies are susceptible to severe recurrent infections, especially from herpesviruses like CMV.[5,6]

miRNAs are ~ 22-nt noncoding RNAs generated from long RNA precursors by serial cleavage steps mediated by the Drosha-DGCR8 complex and Dicer. NK and T cells that lack miRNAs because of the targeted inactivation of *Dicer*, *Drosha*, or *DGCR8* show dramatic defects in proliferation, survival, and effector function.[7,8] In addition, mutations in specific miRNAs, such as miR-181, miR-150, and miR-155, can have dramatic effects on NK-cell development, cytotoxicity, and IFN-γ production.[9-11] Individual miRNAs can modestly affect the stability and translation of hundreds of target mRNAs.[12,13] Because multiple miRNAs may regulate the same biologic processes, posttranscriptional regulation of miRNAs as a class may profoundly alter gene expression programs.[14]

Eri1 is a 3′-to-5′ exoribonuclease of the DEDDh family with a deeply conserved role in 5.8S rRNA 3′ end processing.[15,16] It has also been repeatedly recruited into species-specific small RNA regulatory pathways over the course of evolution. *eri1* mutant *Schizosaccharomyces pombe* accumulate excess endogenous short-interfering RNAs (endo-siRNAs) that promote heterochromatin formation.[17,18] In contrast, *Caenorhabditis elegans* ERI-1 forms a complex with Dicer that generates worm-specific classes of endo-siRNAs.[19,20] *eri-1* mutant worms lack these endo-siRNAs, but also display an enhanced RNAi (Eri) phenotype whereby exogenous siRNAs show more robust silencing of mRNA targets.[21] Eri1 overexpression suppresses RNAi in mouse and human cell lines,[22] but its role in mammalian endogenous small RNA pathways remains undefined. Here, we report that Eri1 negatively regulates global miRNA abundance and is required to promote normal NK-cell homeostasis and immune function.

Methods

Mice and infections

C57BL/6 (JAX; B6), CD45.1^{+} (*Ptprc*$^{a/a}$) B6 (NCI), ICR, and *Rag2*$^{-/-}$*Il2rg*$^{-/-}$ mice (Taconic) were purchased. *Eri1*$^{fl/fl}$;*CD4-cre*, *Eri1*$^{-/-}$, and Ly49H-deficient (*Klr8*$^{-/-}$) B6 mice were described previously.[15,23] ICR/B6 mice

Submitted November 21, 2011; accepted May 13, 2012. Prepublished online as *Blood* First Edition paper, May 21, 2012; DOI 10.1182/blood-2011-11-394072.

The online version of this article contains a data supplement.

The publication costs of this article were defrayed in part by page charge payment. Therefore, and solely to indicate this fact, this article is hereby marked "advertisement" in accordance with 18 USC section 1734.

were generated by crossing ICR to *Eri1*$^{+/-}$ B6 mice and backcrossing F_1 mice to *Eri1*$^{+/-}$ B6. To create chimeras, embryonic day 14.5 fetal liver cells were harvested and injected intravenously into B6 mice lethally irradiated with a split dose of 1100 rad. For infections, mice were injected intraperitoneally with 5×10^4 PFU MCMV (Smith Strain). All experiments were conducted in accordance with the University of California, San Francisco Institutional Animal Care and Use Committee (IACUC) guidelines with approval from the university IACUC.

NK cytokine production and cytotoxicity

Splenic NK cells were stimulated with Abs against NK1.1, NKp46, Ly49D, Ly49H, or rat IgG2a or were incubated with IL-12 (20 ng/mL) and IL-18 (10 ng/mL; R&D Systems). For LAMP-1 analysis, stimulated NK cells were incubated with anti-CD107a Ab (1D4B; eBioscience). Splenocytes were incubated on Ab-coated plates for 5 hours in the presence of Brefeldin A followed by intracellular cytokine staining for IFN-γ. For cytotoxicity assays, wild-type (WT) and *Eri1*$^{-/-}$ NK1.1$^+$ TCRβ$^-$ NK cells were incubated for 6 hours with Ba/F3 cells or Ba/F3 cells stably expressing m157.[3] ^{51}Cr release was used as described to measure NK cell–mediated lysis.[24]

Western blot

Splenic NK1.1$^+$TCRβ$^-$Ly49H$^+$ cells from uninfected or MCMV-infected B6 mice were sorted using a FACSAria (BD Biosciences). Western blots were performed using a mAb against β-actin (AC-74; Sigma Aldrich) and an affinity-purified polyclonal Ab against Eri1 (A28).[15]

Adoptive transfers

Congenically marked WT and *Eri1*$^{-/-}$ B6 splenic Ly49H$^+$ NK cells were mixed at a 1:1 ratio, labeled with 10μM CellTrace Violet as per the manufacturer's instructions (Invitrogen), and 6×10^4 Ly49H$^+$ NK equivalents were transferred intravenously into Ly49H-deficient recipients. Twenty-four hours later, mice were injected with MCMV. Alternatively, WT and *Eri1*$^{-/-}$ B6 splenic NK cells were mixed at a 1:1 ratio, and 0.5×10^6 NK equivalents were transferred intravenously into *Rag2*$^{-/-}$*Il2rg*$^{-/-}$ B6 mice.

MCMV titers

Unmixed chimeras were infected with MCMV and euthanized 3.5 days later. Splenic and hepatic viral titers were determined as described previously.[24]

T-cell culture and stimulation

CD4$^+$ T cells were purified from spleen and lymph nodes by magnetic bead selection (Dynal; Invitrogen) and activated with anti-CD3 and anti-CD28 Abs. Cells were taken off stimulus on day 3 and expanded in IL-2–containing media for sorting and analysis on day 6. Splenic T cells from MCMV-infected mice (day 8 postinfection [p.i.]) were isolated and stimulated with MCMV peptides (supplemental Table 1, available on the *Blood* Web site; see the Supplemental Materials link at the top of the online article) or 10 nM phorbol 12-myristate 13-acetate (PMA) and 1μM ionomycin and stained for intracellular IFN-γ as described previously.[25]

MicroRNA microarrays

Purified CD4$^+$ T cells from one *Eri1*$^{-/-}$ and 2 *Eri1*$^{fl/fl}$;*CD4-cre* mice and WT littermate controls (*Eri1*$^{+/+}$, *Eri1*$^{fl/fl}$, and *Eri1*$^{+/+}$;*CD4-cre*) were activated in vitro for 40 hours under Th2 (1000 U/mL IL4 and 5 μg/mL anti–IFN-γ) conditions. Total RNA was isolated (miRNeasy kit; QIAGEN) and used for miRNA analysis using custom one-color Agilent microarrays (8×15K Agilent UCSF Custom miRNA V3.1) containing sequences from Sanger miRBase Version 11.[26] For each set of 5 replicated probes across arrays, $\log_2$-scale average intensities were determined, corrected for background, and quantile-normalized. The false discovery rate was calculated as described.[27]

Deep sequencing

Small (18-30 bp) RNA libraries were constructed from activated ICR/B6 WT and *Eri1*$^{-/-}$ CD4$^+$ T cells and sequenced as described.[28] Adaptor sequences were trimmed from reads as described,[29] and all reads 15-30 nt were mapped to the mouse genome (UCSC mm8 assembly). Only sequences mapping to the genome with up to 2 mismatches were analyzed. Mouse small noncoding RNA annotations were compiled as described.[30] For genome-wide analysis, sequences were grouped into independent genomic loci as described,[29] and relative reads from each library were compared at every locus. Using an empirical Bayes method,[31] we determined that loci with a posterior probability > 0.9 of ≥ 5-fold change were determined to have significantly differential expression.

Accession numbers

Deep sequencing (GSE31920) and microarray (GSE32126) data are available in the Gene Expression Omnibus (GEO) database.

Results

Peripheral deficiency and impaired BM expansion of *Eri1*$^{-/-}$ NK cells

Compared with other tissues, Eri1 is highly expressed in mouse spleen and thymus, suggesting a role in the immune system.[15] To determine whether the absence of Eri1 alters mature immune cell homeostasis, we evaluated splenocyte population frequencies in WT and Eri1-deficient (*Eri1*$^{-/-}$) animals. The frequency and number of NK cells in the spleens of *Eri1*$^{-/-}$ animals was reduced by 50% compared with their WT siblings (Figure 1A-B). Other lymphocyte populations were present at normal numbers. NK-cell frequency was also significantly reduced in the liver ($P < .01$) and BM ($P < .05$; Figure 1C). Similar results were obtained in hematopoietic chimeras reconstituted with WT or *Eri1*$^{-/-}$ E14.5 fetal liver cells (supplemental Figure 1). Thus, *Eri1*$^{-/-}$ NK-cell reduction is intrinsic to the hematopoietic compartment.

We next considered the possibility that the decrease in *Eri1*$^{-/-}$ NK cells results from dysfunction in other hematopoietic cells. To test this hypothesis, we generated chimeras using a 1:1 mixture of *Eri1*$^{+/+}$ (CD45.1$^+$CD45.2$^+$) and *Eri1*$^{-/-}$ (CD45.1$^-$CD45.2$^+$) E14.5 fetal liver cells. Mixed chimeras contained similar frequencies of BM *Eri1*$^{+/+}$ and *Eri1*$^{-/-}$ Lin$^-$Sca-1$^+$c-Kit$^+$ early hematopoietic precursors (Figure 1D); yet, we observed a significant reduction in all splenic *Eri1*$^{-/-}$ lymphocyte lineages, including but not limited to NK cells (Figure 1D-E). In contrast, *Eri1*$^{+/+}$ and *Eri1*$^{-/-}$ splenic myeloid cell frequencies were similar. Because the presence of WT hematopoietic cells did not rescue the reduction in *Eri1*$^{-/-}$ NK cells, we conclude that Eri1 is required in a cell-intrinsic manner to maintain normal NK-cell numbers. Furthermore, competitive reconstitution unmasked a general defect in *Eri1*$^{-/-}$ lymphocyte homeostasis that was not apparent in *Eri1*$^{-/-}$ mice (Figure 1A-B). This may reflect defective peripheral turnover because of competition for limiting growth factors or reduced development from a common lymphocyte precursor.

Developing BM NK cells undergo ordered stages of maturation marked by the up-regulation or down-regulation of specific integrins and the acquisition of NK receptors.[32] We examined 5 discrete populations of developing *Eri1*$^{+/+}$ and *Eri1*$^{-/-}$ BM NK cells in mixed fetal liver chimeras (Figure 1F, supplemental Figure 2A). There were no differences in the relative frequencies of *Eri1*$^{+/+}$ and *Eri1*$^{-/-}$ cells among early NK-cell precursors (stages I-III). However, *Eri1*$^{-/-}$ NK cells were significantly reduced starting at

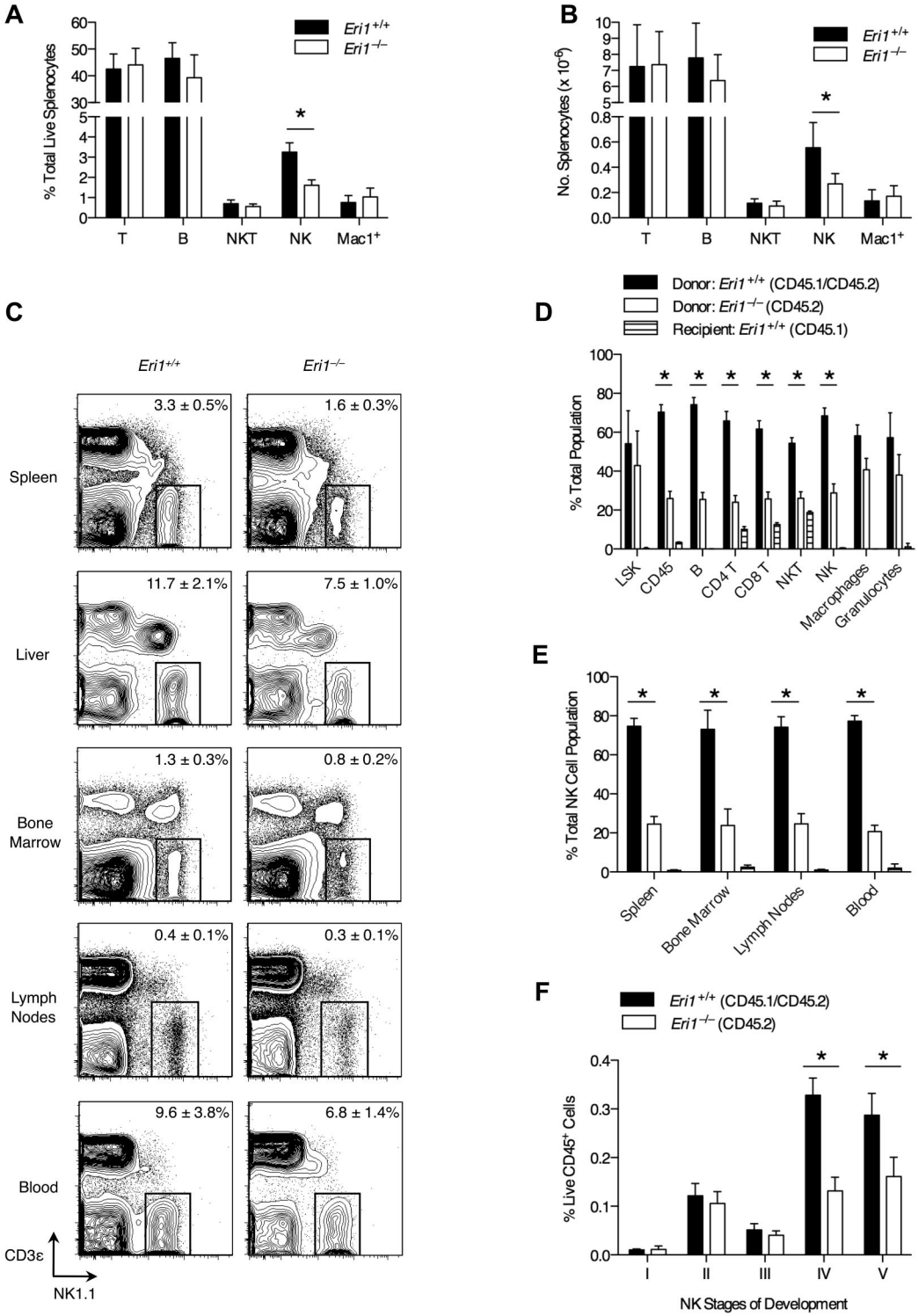

Figure 1. NK-cell deficiency in *Eri1*$^{-/-}$ mice. (A) Frequency and (B) absolute number of spleen T (CD3ε$^+$NK1.1$^-$), B (CD19$^+$), NKT (NK1.1$^+$CD3ε$^+$), NK (NK1.1$^+$CD3ε$^-$), and Mac1$^+$ (CD11b$^+$NK1.1$^-$) cells enumerated by flow cytometry (N = 5, ICR/B6 mice). (C) NK1.1$^+$CD3ε$^-$ NK cells in the indicated tissues. Numbers are NK-cell frequency ± SD among total lymphocytes (N = 5, ICR/B6 mice). (D-F) CD45.1$^+$ lethally irradiated hosts were reconstituted with a 1:1 mixture of fetal liver cells from WT (CD45.1$^+$ CD45.2$^+$) and *Eri1*$^{-/-}$ (CD45.2$^+$) donors and analyzed 8-15 weeks later (N = 3). (D) Frequency of donor- and host-derived cells among BM LSK (Lin$^-$c-Kit$^+$ Sca-1$^+$) cells and spleen CD45$^+$, B, CD4$^+$ and CD8$^+$ T, NKT, NK, macrophage (CD11b$^+$NK1.1$^-$Gr1$^-$), and granulocyte (CD11b$^+$ Gr1$^+$) cells. (E) Frequency of donor- and host-derived cells among NK cells in the indicated tissues. (F) Frequency of developing NK-cell subsets (see supplemental Figure 2A for gating strategy) among BM WT (CD45.1$^+$CD45.2$^+$) and *Eri1*$^{-/-}$ (CD45.1$^-$CD45.2$^+$) cells. Bar graphs show mean ± SD; $^*P \leq .05$, (A-B) unpaired or (D-F) paired Student *t* test. All data are representative of at least 2 independent experiments.

stage IV, which corresponds with a major proliferative phase, and at stage V, which is equivalent to mature CD11b$^+$ NK cells. Although an underlying mechanism remains unclear, these data indicate that inefficient production of *Eri1*$^{-/-}$ NK cells in the BM contributes to their inability to populate peripheral compartments at normal frequencies.

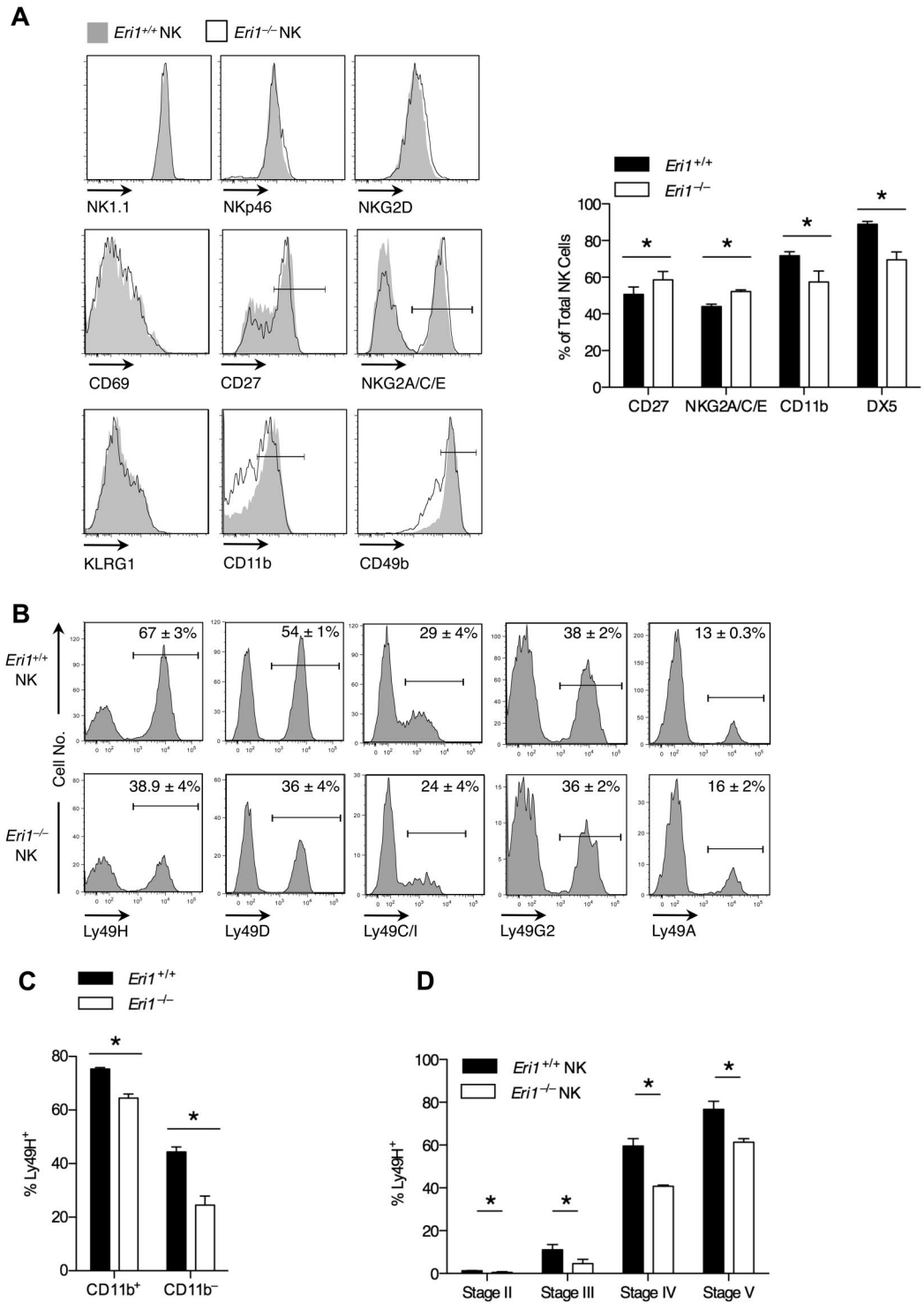

Figure 2. Impaired maturation and Ly49 receptor expression in *Eri1*$^{-/-}$ NK cells. B6 WT CD45.1$^+$ lethally irradiated hosts were reconstituted with a 1:1 mixture of congenic WT (CD45.1$^+$CD45.2$^+$) and *Eri1*$^{-/-}$ (CD45.2$^+$) fetal liver cells. (A-C) Splenic and (D) BM NK cells were analyzed by flow cytometry at 8-15 weeks. (A) Cell-surface expression of activating receptors (NKp46 and NK1.1), activation markers (NKG2D and CD69), and maturation markers (CD27, NKG2A/C/E, KLRG1, CD11b, and CD49b) on WT (CD45.1$^+$CD45.2$^+$) and *Eri1*$^{-/-}$ (CD45.1$^-$CD45.2$^+$) cells (left). Gated NK1.1$^+$CD3ϵ^- cells are shown for all stains, except for NK1.1, which shows gating on NKp46$^+$TCRβ^- cells. Summary of markers with significantly different expression on WT and *Eri1*$^{-/-}$ NK cells (right). (B) Splenic NK-cell activating and inhibitory Ly49 receptors. (C) Percentage of Ly49H$^+$ cells among CD11b$^+$ and CD11b$^-$ NK cells. (D) Percentage of Ly49H$^+$ WT and *Eri1*$^{-/-}$ NK cells at various stages of NK-cell maturation in the BM (gating shown in supplemental Figure 2A). Bar graphs and flow cytometry plots show mean ± SD (N = 3 mice). *$P \leq .05$; paired Student *t* test.

Further analysis of developing WT BM NK populations revealed that stage III NK cells displayed high rates of cell death and apoptosis before they up-regulated CD49b and underwent a major proliferative burst at stage IV (supplemental Figure 2B-D). WT and *Eri1*$^{-/-}$ NK populations displayed similar frequencies of dead and apoptotic cells during all stages of BM development (supplemental Figure 2B-C). Eri1 deficiency also did not affect the frequency of BrdU-labeled cells after a 3- or 16-hour pulse (supplemental Figure 2D, data not shown). Rapid clearance of necrotic and apoptotic cells in vivo may preclude the detection of subtle differences in cell

Table 1. Activating and inhibitory receptor repertoire on splenic and developing BM NK cells

	Eri1	II	III	IV	V	Spleen
Ly49H	+/+	1.3 (0.1)	11.0 (2.5)	59.6 (3.4)	76.7 (3.8)	71.0 (3.5)
	−/−	0.5 (0.3)	4.6 (2.0)	40.8 (0.6)	61.4 (1.7)	50.1 (3.5)
Ly49D	+/+	2.8 (0.5)	13.6 (2.0)	54.6 (2.9)	55.4 (1.5)	59.2 (1.0)
	−/−	2.3 (0.7)	6.9 (1.8)	47.7 (1.8)	53.1 (1.6)	48.4 (1.4)
Ly49G2	+/+	4.2 (1.6)	15.9 (3.1)	50.4 (5.6)	49.2 (4.9)	37.3 (2.7)
	−/−	4.2 (1.6)	10.2 (2.4)	56.6 (2.3)	56.0 (5.2)	38.1 (6.0)
Ly49C/I	+/+	5.5 (0.7)	19.0 (4.9)	30.9 (1.2)	34.6 (1.1)	28.9 (3.5)
	−/−	3.5 (1.2)	7.4 (1.2)	26.0 (1.7)	30.9 (1.9)	24.4 (4.0)
NKG2A/C/E	+/+	59.8 (0.7)	60.1 (2.0)	44.9 (0.7)	45.5 (1.1)	44.0 (1.3)
	−/−	60.7 (3.2)	60.0 (1.8)	55.9 (4.2)	51.8 (2.8)	52.2 (0.9)

WT CD45.1$^+$ lethally irradiated hosts were reconstituted with a 1:1 mixture of fetal liver cells from congenic WT (CD45.1$^+$CD45.2$^+$) and *Eri1*$^{-/-}$ (CD45.2$^+$) mice and analyzed 12 weeks later. Frequencies of NK-cell receptor expression on freshly isolated WT and *Eri1*$^{-/-}$ splenic NK cells (NK1.1$^+$CD3ε$^-$) and stage II-V developing BM NK cells (gating strategy shown in supplemental Figure 2A) are shown. Mean (SD) for 3 mice are listed.

death, and differences in proliferation that occur outside the pulse window may not be detected by BrdU labeling. Nevertheless, we can exclude the possibility that major stage-specific differences in cell death and proliferation underlie the cell-intrinsic reduction of *Eri1*$^{-/-}$ BM NK cells.

Given the relatively large reduction in peripheral NK-cell numbers compared with the BM, we tested whether *Eri1*$^{-/-}$ NK cells have a homeostatic defect that exists independently of developmental impairment. WT and *Eri1*$^{-/-}$ NK cells incorporated BrdU provided in drinking water at the same rate, indicating normal NK-cell turnover at steady state in vivo (supplemental Figure 3A). *Eri1*$^{-/-}$ NK cells also expanded at the same rate as WT cells when transferred into lymphocyte-deficient *Rag2*$^{-/-}$*Il2rg*$^{-/-}$ mice (supplemental Figure 3B). Constitutive signaling through the IL-15 receptor is essential for NK-cell development and survival.[33] WT and *Eri1*$^{-/-}$ NK cells cultured in IL-15 ex vivo proliferated rapidly and underwent similar rates of cell death upon IL-15 withdrawal (supplemental Figure 3C-D). Thus, *Eri1*$^{-/-}$ NK cells are competent to signal through the IL-15 receptor and are not particularly sensitive to the proapoptotic effects of IL-15 withdrawal. Together, these data suggest that *Eri1*$^{-/-}$ NK cells undergo impaired production in the BM in the setting of normal peripheral turnover and IL-15–dependent proliferation.

Impaired maturation and Ly49 receptor expression in Eri1-deficient NK cells

We examined the cell-surface phenotype of *Eri1*$^{-/-}$ and WT NK cells in mixed chimeras to determine whether Eri1 deficiency affects NK-cell maturation or activation status (Figure 2A). *Eri1*$^{-/-}$ NK cells expressed normal levels of the activating receptors NK1.1 and NKp46, which are used to identify the NK lineage. They also expressed normal levels of NKG2D and CD69, which are up-regulated acutely in activated cells, and KLRG1, which remains elevated on NK cells previously expanded by activation.[34] A significantly higher frequency of *Eri1*$^{-/-}$ NK cells expressed the immature cell markers CD27 and NKG2A/C/E, and fewer *Eri1*$^{-/-}$ NK cells expressed CD49b and CD11b, which are up-regulated in the final stages of NK-cell maturation. Similar expression patterns were observed in *Eri1*$^{-/-}$ NK cells from unmixed chimeras (data not shown).

Eri1-deficient NK cells also displayed a skewed Ly49 receptor repertoire (Figure 2B). Surprisingly, *Eri1*$^{-/-}$ NK-cell populations displayed a specific reduction in the frequency of Ly49H- and Ly49D-expressing cells. In contrast to these activating receptors, the inhibitory receptors Ly49C/I, Ly49G2, and Ly49A were expressed normally. Within each Ly49$^+$ subset, WT and *Eri1*$^{-/-}$ NK cells displayed no difference in the intensity of Ly49 receptor staining. Because activating Ly49 receptors are more frequently expressed on mature than immature NK cells, we considered the possibility that reduced Ly49H expression frequency could simply reflect the altered maturation status of *Eri1*$^{-/-}$ NK cells. However, Ly49H expression was decreased among both mature CD11b$^+$ and immature CD11b$^-$ *Eri1*$^{-/-}$ NK cells (Figure 2C), indicating that this defect may occur independently of NK-cell maturation.

During their development, NK cells acquire Ly49 receptors in response to signals from the BM stroma.[35,36] To determine when in NK-cell development *Eri1*$^{-/-}$ NK cells first show reduced Ly49H expression, we measured Ly49H$^+$ NK-cell frequencies among stage II-V cells in the BM of mixed chimeras. Immature CD49b$^-\alpha_V{}^+$ NK cells acquire Ly49 receptors as they up-regulate c-Kit, which demarcates the transition from stage II to III cells (supplemental Figure 2A). *Eri1*$^{-/-}$ NK cells showed a marked reduction in Ly49H$^+$ NK frequency at each developmental stage (Figure 2D). Furthermore, all measured Ly49 receptors, but not NKG2A/C/E receptors, were decreased in stage III *Eri1*$^{-/-}$ NK cells, including inhibitory receptors (Table 1). The inhibitory Ly49 repertoire normalizes in peripheral *Eri1*$^{-/-}$ NK cells, perhaps reflecting a selective growth advantage for NK cells with specific Ly49 repertoires. Together, these data indicate that peripheral *Eri1*$^{-/-}$ NK populations have an immature cell-surface phenotype and a skewed Ly49 repertoire with fewer Ly49 activating receptors.

Eri1 is dispensable for Ly49H-dependent NK cell–mediated cytotoxicity

Activated NK cells degranulate and produce large amounts of IFN-γ. We measured IFN-γ production and the degranulation marker LAMP-1 (CD107a) in freshly isolated splenocytes activated with inflammatory cytokines or plate-bound Abs that ligate activating NK-cell receptors. WT and *Eri1*$^{-/-}$ cells from mixed chimeras were stimulated together, negating indirect feedback mechanisms on NK-cell activation. WT and Eri1-deficient NK cells showed similar LAMP-1 staining in all conditions tested except for ligation of Ly49H (Figure 3A). In contrast, *Eri1*$^{-/-}$ NK cells displayed modestly reduced IFN-γ expression upon cross-linking of all ITAM-associated receptors tested (Figure 3B). More significant decreases were observed with Ly49H and Ly49D cross-linking (35% and 20%, respectively). These results likely reflect the reduced frequency of *Eri1*$^{-/-}$ NK cells expressing these receptors

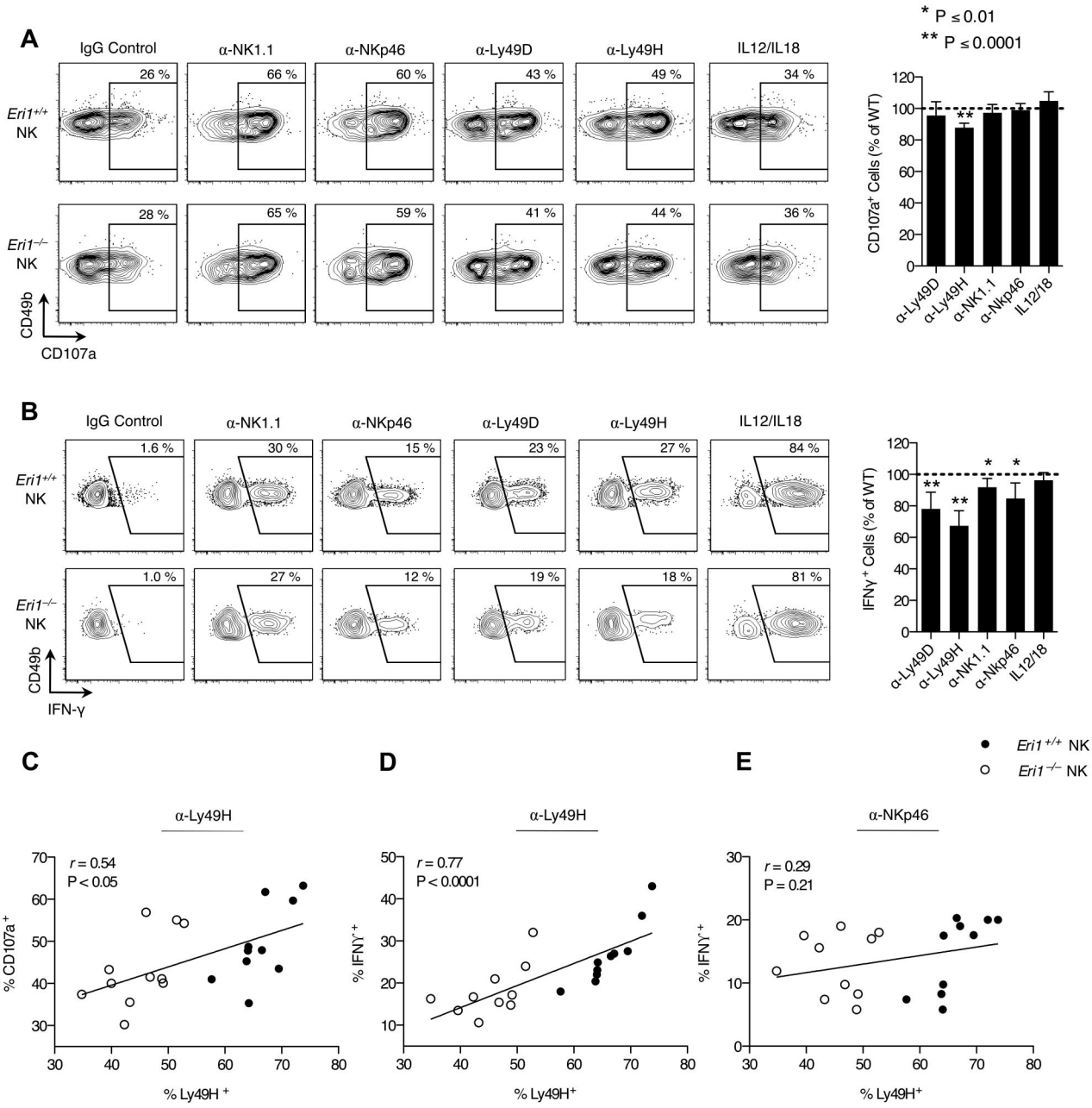

Figure 3. Normal Ly49H-dependent NK-cell cytotoxicity in the absence of Eri1. B6 WT CD45.1$^+$ lethally irradiated hosts were reconstituted with a 1:1 mixture of congenic WT (CD45.1$^+$CD45.2$^+$) and *Eri1*$^{-/-}$ (CD45.2$^+$) fetal liver cells. (A) At 12 weeks, splenocytes were isolated and incubated in wells coated with IgG or mAbs against NK1.1, NKp46, Ly49D, or Ly49H in the presence of anti-CD107a mAb. Alternatively, NK cells were stimulated with IL-12 and IL-18. Frequency of degranulated WT (CD45.1$^+$CD45.2$^+$) and *Eri1*$^{-/-}$ (CD45.1$^-$CD45.2$^+$) CD107a$^+$ NK cells (CD49b$^+$TCRβ$^-$) is shown. (B) Splenic NK cells stimulated as in panel A in the presence of brefeldin A and stained for intracellular IFN-γ. Flow cytometry plots show mean values for 10 mice. Summary graphs for *Eri1*$^{-/-}$ NK (right) show mean relative to WT ± SD (paired Student *t* test). (C-E) Regression of CD107a (C) or IFN-γ (D-E) expression on percentage of Ly49H$^+$ NK cells after stimulation with indicated mAbs. The Pearson correlation coefficient (*r*) and significance test for nonzero correlation (*P*) are shown for each plot (N = 10 mice from 3 independent experiments).

rather than specific effects on Ly49 signaling. Indeed, starting Ly49H$^+$ NK-cell frequency significantly correlated with both LAMP-1 and IFN-γ induction by Ly49H, but not NKp46 cross-linking (Figures 3C-E). In addition, a consistent ~ 35% reduction in the frequency of IFN-γ–producing NK cells was observed when the Ly49H cross-linking Ab stimulus was titrated down over 2 orders of magnitude (data not shown).

To test whether *Eri1*$^{-/-}$ NK cells can efficiently kill target cells in a Ly49H-dependent manner, we incubated freshly isolated NK cells ex vivo with Ba/F3 cells stably transduced with the MCMV Ly49H ligand m157. WT and *Eri1*$^{-/-}$ NK cells lysed the parental Ba/F3 line at similar rates (Figure 4A). Furthermore, WT and *Eri1*$^{-/-}$Ly49H$^+$ NK cells lysed Ba/F3-m157 targets at equal efficiency (Figure 4B). Together, these data indicate that *Eri1*$^{-/-}$ NK cells are competent to signal through NK-cell receptors and mediate normal Ly49H-dependent and -independent cytotoxicity. However, the reduced frequency of Ly49H$^+$ cells in *Eri1*$^{-/-}$ NK-cell populations leads to proportional defects in Ly49H-dependent effector activities.

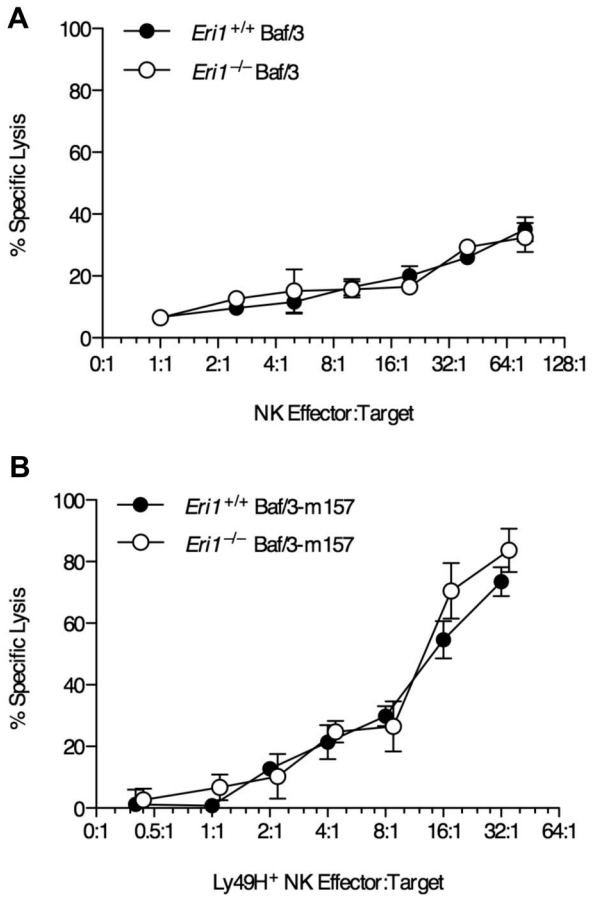

Figure 4. Normal NK-mediated killing in the absence of Eri1. Lethally irradiated CD45.1$^+$ mice were reconstituted with CD45.2$^+$ B6 WT or *Eri1*$^{-/-}$ fetal liver cells. Ten weeks later, splenic NK cells pooled from 3-4 mice were incubated with ^{51}Cr-labeled target (A) Ba/F3 cells or (B) Ba/F3 cells stably expressing MCMV m157. Error bars indicate SD for triplicate measurements. Data are representative of 2 independent experiments.

Eri1$^{-/-}$ NK cells expand less during MCMV infection and show poor control of viral load

Ly49H$^+$ NK cells are critical for controlling MCMV infection in B6 mice.[37,38] Given the reduced Ly49H expression in *Eri1*$^{-/-}$ NK-cell populations, we investigated the in vivo activation of *Eri1*$^{-/-}$ NK cells by MCMV. Early in MCMV infection all NK cells are activated nonspecifically by proinflammatory cytokines such as IL-12, IL-18, and type I IFNs.[39,40] Then, several days after infection, there is marked expansion of Ly49H$^+$ NK cells driven directly by Ly49H ligation by the viral antigen m157.[3,4] Eri1 is strongly up-regulated in Ly49H$^+$ NK cells over the course of MCMV infection (Figure 5A), suggesting a potential role in NK-cell activation. To study *Eri1*$^{-/-}$ NK-cell activation in response to MCMV, we infected mixed chimeras, obviating discrepant cytokine environments or antigenic loads that could complicate experiments in separate WT and *Eri1*$^{-/-}$ mice.

Early in MCMV infection, both WT and *Eri1*$^{-/-}$ NK cells responded with robust IFN-γ production (Figure 5B) and up-regulation of NKG2D and CD69 (Figure 5C). These results are consistent with efficient IFN-γ production upon IL-12 and IL-18 stimulation ex vivo (Figure 3B). Later in MCMV infection, WT Ly49H$^+$ NK cells showed robust expansion, peaking at day 7 in both spleen and liver (Figure 5D). In contrast, *Eri1*$^{-/-}$ Ly49H$^+$ NK cells underwent inefficient expansion. As expected, Ly49H$^-$ NK cells showed little change in total cell number regardless of their genotype. To assess *Eri1*$^{-/-}$ NK-cell expansion independent of the reduced initial Ly49H$^+$ cell frequency, we adoptively transferred equal numbers of CellTrace Violet–labeled WT and *Eri1*$^{-/-}$ Ly49H$^+$ NK cells into Ly49H-deficient hosts. Four days after infection with MCMV, WT Ly49H$^+$ NK cells had diluted the cell proliferation dye more and undergone greater expansion than *Eri1*$^{-/-}$ cells (Figure 5E-F). Thus, Eri1-deficient NK cells are activated normally in early MCMV infection yet undergo poor Ly49H-dependent proliferation as the infection progresses.

To determine whether Eri1 is required to control viral load, we infected unmixed chimeras with MCMV. As observed in mixed chimeras, *Eri1*$^{-/-}$ NK cells showed robust expression of IFN-γ and up-regulated the early activation markers CD69 and NKG2D yet displayed reduced expansion of Ly49H$^+$ cells (data not shown). Like other mice with poor NK-cell expansion,[6,23] *Eri1*$^{-/-}$ chimeras exhibited decreased splenomegaly and increased viral titers (Figure 5G-H). We conclude that Eri1 is required in a cell-intrinsic manner for the normal expansion of Ly49H$^+$ NK cells and control of MCMV infection.

Reduced virus-specific T-cell responses in the absence of Eri1

Unlike NK cells, CD4 and CD8 lineage T cells were present at normal steady-state numbers and proportions in the thymus and peripheral lymphoid tissues of *Eri1*$^{-/-}$ fetal liver chimeras (data not shown, supplemental Figure 1A). The proportions of naive, memory, and regulatory T cells were also normal, and similar results were obtained in *Eri1*$^{fl/fl}$;*CD4-cre* mice that lack Eri1 only in T cells (data not shown). However, given the more general defect in *Eri1*$^{-/-}$ lymphocyte development revealed in mixed fetal liver chimeras and the decreased expansion of Ag-specific *Eri1*$^{-/-}$ NK cells during MCMV infection, we examined MCMV-specific responses in *Eri1*$^{-/-}$ CD4$^+$ and CD8$^+$ T cells in mixed fetal liver chimeras.

At day 8 p.i., T cells were evaluated by flow cytometry and by restimulation ex vivo with immunodominant MCMV peptides.[25,41] As expected, infection increased the overall frequency of CD8$^+$ T cells (Figure 6A) and the proportion of activated CD4$^+$ and CD8$^+$ T cells marked by high expression of CD44 and/or down-regulation of CD62L (Figure 6B). These changes occurred similarly in WT and *Eri1*$^{-/-}$ T cells (Figure 6A-B). However, fewer *Eri1*$^{-/-}$ CD8$^+$ cells were specific for the H2-D^b–restricted M45$_{985\text{-}993}$ peptide epitope (Figure 6C). Accordingly, M45 induced fewer IFN-γ–producing *Eri1*$^{-/-}$ CD8$^+$ cells, despite their increased response to PMA and ionomycin (Figure 6D-E). We also detected a reduced frequency of MCMV-specific IFN-γ–producing *Eri1*$^{-/-}$ CD4$^+$ T cells despite robust IFN-γ production on PMA and ionomycin restimulation (Figure 6F-G). Together, these data indicate that, like NK cells, *Eri1*$^{-/-}$ T cells have diminished Ag-specific responses to MCMV infection. This defect is unlikely to contribute to poor MCMV control in *Eri1*$^{-/-}$ chimeras at day 3 p.i. (Figure 5H), when T cells, as well as B and NKT cells, are dispensable for viral clearance.[42] However, decreased antiviral T-cell responses in the absence of Eri1 may have important functional consequences for the control of latent infection and the establishment of MCMV-specific immunologic memory.

Eri1 negatively regulates miRNA abundance in lymphocytes

We next sought to identify important RNA targets for Eri1 in mouse lymphocytes. Eri1 inhibits RNAi in worms and mammalian cell lines and degrades siRNA duplexes in vitro.[21,22] Given structural

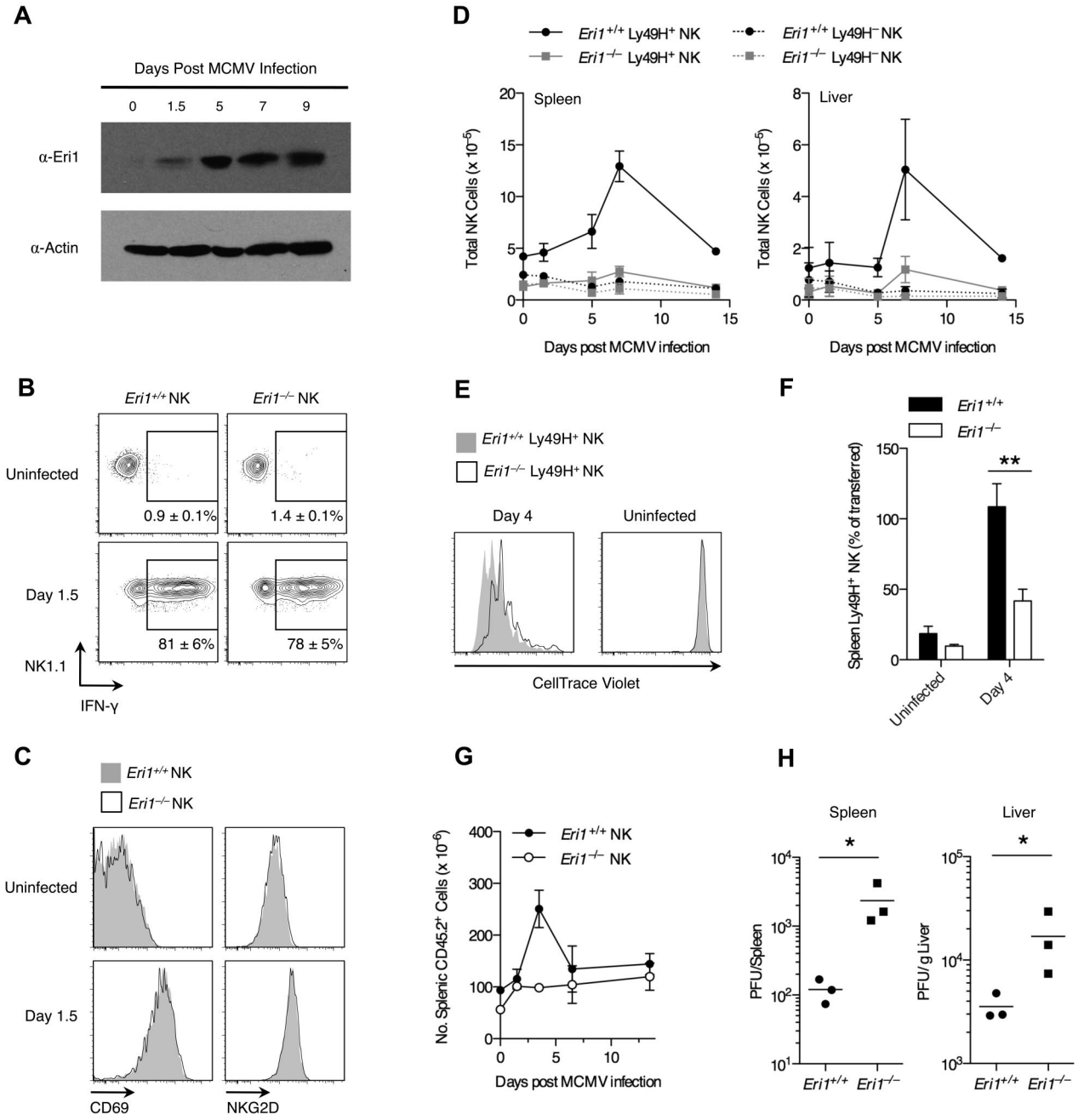

Figure 5. Eri1 is required for Ly49H$^+$ NK-cell expansion and control of viral titers in MCMV infection. (A) Anti-Eri1 mAb immunoblot of Ly49H$^+$ NK cells pooled from 3-4 mice and sorted at various time points after MCMV infection. Data are representative of 2 independent experiments. (B-D) B6 WT CD45.1$^+$ lethally irradiated hosts were reconstituted with a 1:1 mixture of congenic WT (CD45.1$^+$ CD45.2$^+$) and *Eri1*$^{-/-}$ (CD45.2$^+$) fetal liver cells. At 8-15 weeks, chimeras were infected with MCMV. WT (CD45.1$^+$CD45.2$^+$) and *Eri1*$^{-/-}$ (CD45.1$^-$CD45.2$^+$) NK cells (NK1.1$^+$ CD3ε$^-$) were analyzed for (B) intracellular IFN-γ and (C) cell-surface CD69 and NKG2D expression. (D) Absolute numbers of WT and *Eri1*$^{-/-}$ Ly49H$^+$ and Ly49H$^-$ NK cells in the spleen and liver at various time points after infection. Error bars in panels B and D indicate SD (N = 3 mice). (E-F) CD45.2$^+$ *Eri1*$^{-/-}$ splenic Ly49H$^+$ NK cells from reconstituted fetal liver chimeras or B6 mice were mixed 1:1 with splenic Ly49H$^+$ NK cells from CD45.1$^+$CD45.2$^+$ or CD45.1$^+$ WT B6 mice. Mixed splenocytes were labeled with CellTrace Violet and transferred into B6 CD45.1$^+$ *Ly49H*$^{-/-}$ hosts. (E) CellTrace Violet dilution before and after MCMV infection. (F) Percentage of Ly49H$^+$ NK cells transferred at day 0 (mean ± SEM, N = 13 infected and 4 uninfected mice from 4 independent experiments). $^{**}P \leq .001$, paired Student *t* test. (G-H) B6 WT CD45.1$^+$ lethally irradiated hosts were reconstituted with CD45.2$^+$ WT or *Eri1*$^{-/-}$ fetal liver cells and infected with MCMV at 12 weeks. (G) Absolute numbers of WT and *Eri1*$^{-/-}$ CD45.2$^+$ splenocytes over the course of infection (mean ± SD, N = 3 mice). (H) Viral titers in the spleen and liver were determined at day 3.5 p.i. by plaque assays. Horizontal line indicates the mean of each group (N = 3 mice). $^{*}P \leq .05$; 2-tailed Mann-Whitney *U* test.

similarities between miRNA and siRNA duplexes, we conjectured that Eri1 regulates miRNA abundance in lymphocytes. Indeed, quantitative real-time PCR (qRT-PCR) revealed, on average, a 2-fold increase in miRNA expression in *Eri1*$^{-/-}$ NK cells compared with littermate controls (Figure 7A). Highly expressed miRNAs (eg, miR-150 and miR-21) and those expressed at 1-2 lower orders of magnitude (eg, miR-106a and miR-181) were affected.[43] Other noncoding RNAs, including U6 snRNA, U7 snRNA, Arg-tRNA, and Sno202 were unaffected (Figure 7A, data not shown).

Eri1 also regulated miRNA abundance in CD4$^+$ T cells. Northern blot analyses showed a modest, consistent increase in the expression of several miRNAs in Eri1-deficient T cells (Figure

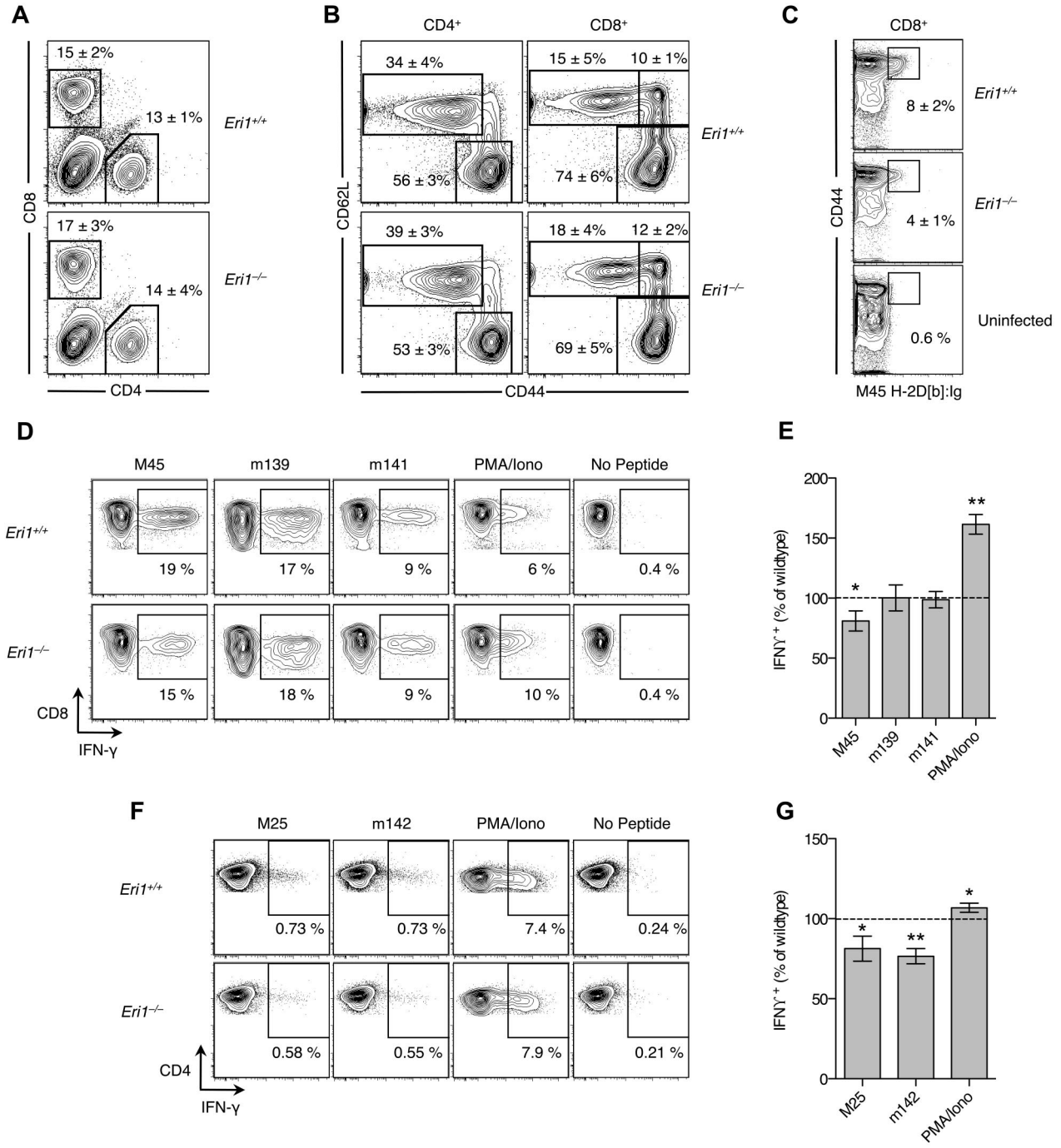

Figure 6. Reduced MCMV-specific CD4$^+$ and CD8$^+$ T-cell frequency in the absence of Eri1. B6 WT CD45.1$^+$ lethally irradiated hosts were reconstituted with a 1:1 mixture of congenic WT (CD45.1$^+$ CD45.2$^+$) and *Eri1*$^{-/-}$ (CD45.2$^+$) fetal liver cells. At 8-15 weeks, chimeras were infected with MCMV and splenocytes were analyzed by flow cytometry at day 8 p.i. (A) Frequency of CD4$^+$ and CD8$^+$ cells among WT (CD45.1$^+$ CD45.2$^+$) or *Eri1*$^{-/-}$ (CD45.1$^-$ CD45.2$^+$) splenocytes. (B) CD44 and CD62L expression on WT and *Eri1*$^{-/-}$ CD4$^+$ and CD8$^+$ cells. (C) Frequency of WT and *Eri1*$^{-/-}$ (day 8 p.i.) or WT control (uninfected) CD8$^+$ cells labeled with M45-loaded H2-D^b:Ig dimer. (D-G) Splenocytes from infected mice were restimulated with indicated peptides or PMA and ionomycin. Flow cytometric plots show the average percentage of gated (D) CD8$^+$ or (F) CD4$^+$ cells producing intracellular IFN-γ. Summary graphs for *Eri1*$^{-/-}$ splenic (E) CD8$^+$ and (G) CD4$^+$ T cells show mean IFN-γ expression relative to WT. Numbers indicate average values (A-C) ± SD or (E,G) SEM for 6 mice from 2 independent experiments. *$P \leq .05$ **$P \leq .001$; unpaired Student *t* test.

7B). Because we could transduce primary *Eri1*$^{-/-}$ T cells more easily than NK cells, we used these lymphocytes to rescue miRNA levels by ectopic expression of Eri1. Transducing Eri1-deficient T cells with a retrovirus encoding an Eri1-ECFP fusion protein[15] reduced miRNA expression to WT levels (Figure 7C). Thus, altered miRNA abundance in Eri1-deficient lymphocytes was not the indirect result of impaired lymphocyte development.

To test whether Eri1 preferentially affects some miRNAs, we performed microarray analysis of 3 independent Eri1-deficient and matched WT control T-cell samples (Figure 7D). Despite a high degree of reproducibility between samples (Pearson correlation coefficient $r \geq 0.99$), this analysis revealed no differentially expressed miRNAs in Eri1-deficient cells when using a false discovery rate of 5%. Note that array data were quantile normalized to

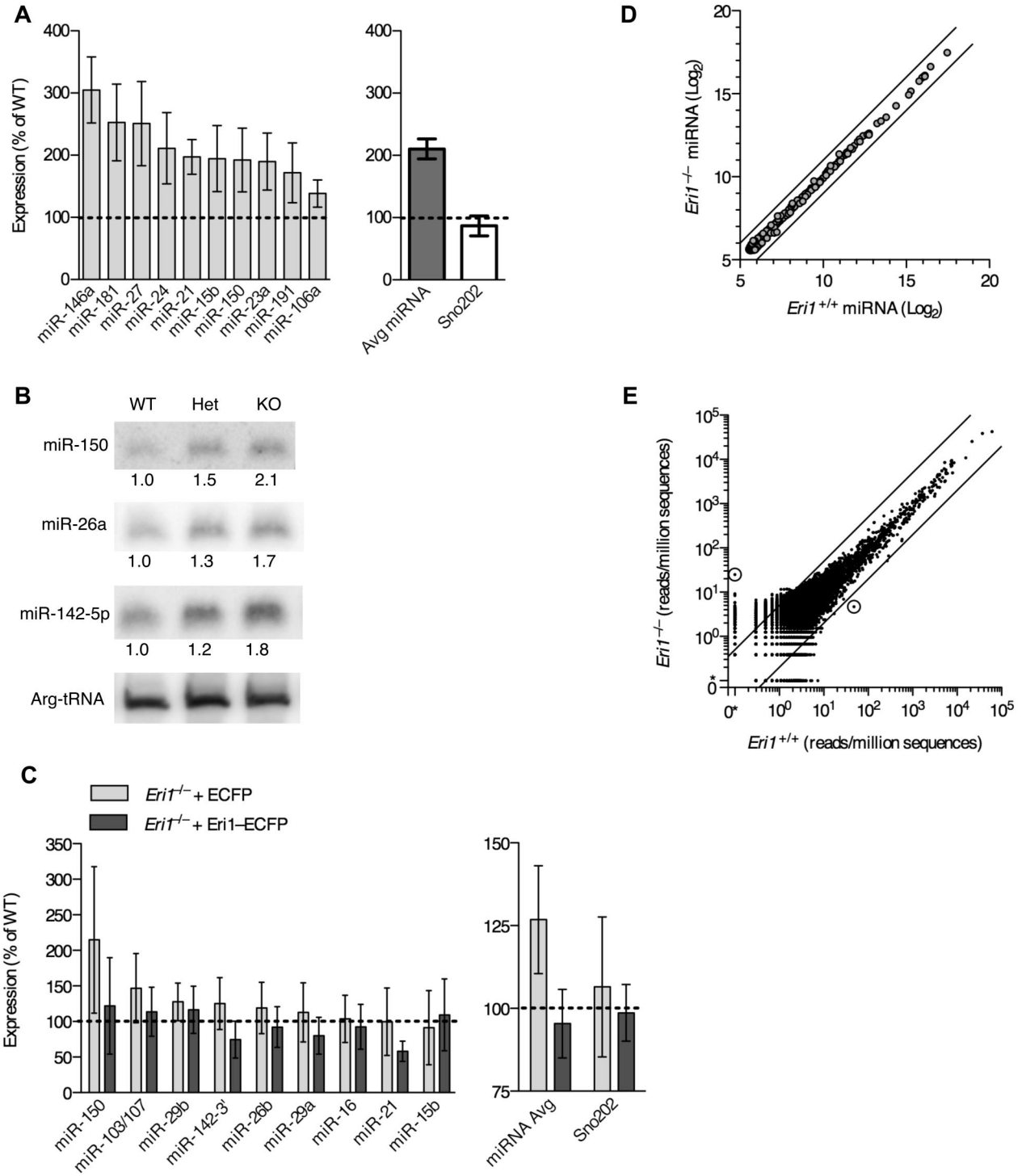

Figure 7. Eri1 negatively regulates miRNAs in lymphocytes. (A) qRT-PCR analysis of miRNA expression in ICR/B6 *Eri1*$^{-/-}$ NK (NK1.1^{+}CD3ϵ^{-}) cells purified by flow cytometry. (Left) miRNA levels in *Eri1*$^{-/-}$ NK cells shown relative to WT (■). (Right) Sum of measurements from 10 miRNAs (■) and Sno202 (□). Data were normalized to U6 snRNA. Graphs indicate mean ± SEM (N = 6, ICR/B6 littermates). (B) Northern blot analysis of miRNAs from Eri1 WT (WT, *Eri1*$^{+/+}$;*CD4-cre*), heterozygous (Het, *Eri1*$^{fl/+}$;*CD4-cre*), and knockout (KO, *Eri1*$^{fl/fl}$;*CD4-cre*) CD4^{+} T cells. Values indicate miRNA-specific signals quantified by phosphoimager, normalized to Arg-tRNA, and expressed relative to WT T cells. (C Left) qRT-PCR analysis of miRNA expression in Eri1-deficient (*Eri1*$^{fl/fl}$;*CD4-cre*) T cells transduced with retroviruses encoding Thy1.1 and ECFP (■) or Thy1.1 and Eri1-ECFP (■). Total RNA was prepared from transduced Thy1.1^{+} T cells purified by FACS. Data were normalized to U6 snRNA and expressed relative to miRNA measured in WT (*Eri1*$^{+/+}$;*CD4-cre*) T cells transduced with ECFP retrovirus. (Right) Average of all miRNAs measured and Sno202 control. Columns show mean ± SEM (4 independent experiments). (D) Microarray comparison of miRNA expression patterns in WT and Eri1-deficient CD4^{+} T cells. Circles show average $\log_2$ hybridization fluorescence intensity values for quantile-normalized data from 3 independent T-cell samples. Black diagonal lines show 2-fold intensity differences. (E) Small RNA read counts from WT and *Eri1*$^{-/-}$ T-cell sequencing libraries. Dots show read counts at independent genomic loci with reads normalized to total genomic sequences in each library. Black lines indicate 5-fold expression differences. Circled dots show loci with > 90% posterior probability of a 5-fold expression difference between libraries. The location of these loci and gene origin of the most frequently cloned RNA from that locus are (left) Chr13:98860450-98860650, *Rps18* pseudogene and (right) Chr8:73490090-73490290, *Ell*.

compare expression of each miRNA relative to all other miRNAs, so these experiments do not detect global changes in miRNA expression. The high degree of similarity in miRNA expression patterns between WT and Eri1-deficient T cells indicated that Eri1 globally regulates the homeostasis of all miRNAs without any discernible sequence specificity.

In *C elegans*, ERI-1 interacts with Dicer to form a complex that is required to generate some classes of endo-siRNAs.[19,20] To determine whether Eri1 is required for the biogenesis of any noncanonical classes of small RNAs in mouse lymphocytes, we used deep sequencing to broadly profile the small RNA transcriptome of WT and *Eri1*$^{-/-}$ T cells (Figure 7E, supplemental Figure 4). All sequences were mapped to the mouse genome and assigned to 390 000 empirically determined genomic loci as described previously.[29] This analysis revealed a high degree of similarity between WT and *Eri1*$^{-/-}$ small RNA libraries ($r > 0.97$; Figure 7E). Only 2 genomic loci had a $> 90\%$ probability of a 5-fold or greater expression difference between the 2 libraries. A 5-fold cutoff for significance was established based on the observation that *C elegans* deficient in components of the ERI-1–Dicer complex show at least a 5-fold decrease in specific classes of endo-siRNAs.[44] Of the 2 loci differentially expressed in Eri1-deficient T cells, one (chromosome 13) could be accounted for by a single nucleotide polymorphism present in the *Eri1*$^{-/-}$ but not the WT sample. The other locus (chromosome 8) contained a 28-nt RNA that mapped to a nonconserved intronic region of *Ell*. Using qRT-PCR, we could not confirm that this RNA was differentially expressed in *Eri1*$^{-/-}$ T cells (data not shown). Together, our small RNA profiling data show that Eri1 negatively regulates miRNA abundance in a sequence-independent manner and that Eri1 is not required for the biogenesis of any abundant classes of small RNAs in T cells.

Discussion

Eri1 is a highly conserved exoribonuclease that has been recruited into small RNA regulatory pathways in evolutionarily diverse organisms. Our findings establish that mammalian Eri1 modulates global miRNA abundance, a novel regulatory activity that may be important for proper lymphocyte development and effector function. While *Eri1*$^{-/-}$ mice had normal numbers of B, T, and NKT cells, all *Eri1*$^{-/-}$ lymphocyte lineages were reduced in mixed fetal liver chimeras. Thus, in the absence of competition, the homeostatic control of peripheral B- and T-cell numbers in *Eri1*$^{-/-}$ mice likely masks a defect in their development. In contrast, steady-state NK-cell populations were reduced to half their normal number. This observation may reflect differences in the regulation of NK-cell versus B- and T-cell homeostasis, or an NK cell–specific dependence on Eri1 activity. The remaining *Eri1*$^{-/-}$ NK cells exhibited an immature phenotype and skewed Ly49 repertoire marked by reduced Ly49H^{+} cells. Furthermore, these *Eri1*$^{-/-}$ Ly49H^{+} NK cells failed to expand efficiently during MCMV infection. *Eri1*$^{-/-}$ CD4^{+} and CD8^{+} T cells also displayed diminished Ag-specific MCMV responses, suggesting that Eri1 may generally enhance lymphocyte-mediated antiviral immunity.

Immature BM CD49b$^{-}\alpha_{V}^{+}$ NK cells acquire Ly49 receptors in a developmentally regulated fashion that correlates with c-Kit up-regulation.[32] Ly49 induction requires direct contact with the BM stroma and is altered in the setting of signaling pathway defects.[35,36,45,46] Similar to NK cells deficient in PI3K subunits or phospholipase Cγ2, *Eri1*$^{-/-}$ BM NK cells showed delayed acquisition of multiple Ly49 receptors. However, unlike these mutants, which show mirrored peripheral Ly49 reduction, *Eri1*$^{-/-}$ NK splenocytes have a normal Ly49 inhibitory repertoire and a selective reduction in Ly49D and Ly49H activating receptors. We hypothesize that the specific reduction in activating receptor repertoires results from delayed acquisition of all Ly49 receptors in the BM followed by the selective outgrowth of NK cells bearing specific inhibitory receptors.

Ly49A, Ly49C, Ly49I, Ly49G2, and Ly49D all recognize class I MHC, and MHC may in turn shape their expression on NK cells.[47] In contrast, the MCMV protein m157 is the only known ligand of Ly49H. The observed decrease in Ly49H- and Ly49D-expressing *Eri1*$^{-/-}$ NK cells from mixed chimeras indicates that a cell-intrinsic mechanism underlies this defect rather than aberrant Ly49 ligand distribution. The adapter molecules DAP10 and DAP12 stabilize activating Ly49 receptors on the cell surface, and loss of either of these proteins leads to reduced Ly49D and Ly49H expression.[24,48] Yet, receptor destabilization is an unlikely mechanism for Ly49 repertoire skewing on *Eri1*$^{-/-}$ NK cells, as they showed no change in receptor density at the cell surface. Another possibility is that Ly49 activating receptors are direct miRNA targets that become down-regulated by miRNA derepression in *Eri1*$^{-/-}$ NK cells. This is also unlikely given that miRNA depletion from mature NK cells does not alter Ly49 expression.[8] A more probable scenario is that Eri1 alters Ly49H and Ly49D acquisition indirectly through effects on Ly49 transcriptional regulators. Such a mechanism has been proposed for aberrant Ly49A acquisition observed in miR-150 mutant mice.[9] Further study of *Eri1*$^{-/-}$ NK cells may provide new insight into the BM signals that drive Ly49 expression in developing NK cells.

The best predictor of effective antiviral immunity to MCMV in B6 mice is the expansion of pathogen-specific NK cells.[3,37,38,49] *Eri1*$^{-/-}$ NK cells displayed a reduced Ly49H^{+} repertoire and poor Ly49H-dependent expansion in response to viral infection, with a corresponding deficiency in viral clearance during the acute phase of infection. Although we observed a decreased frequency of MCMV-specific *Eri1*$^{-/-}$ T cells in mixed fetal liver chimeras, T, B, and NKT cells are dispensable for viral clearance during early acute infection.[42] Therefore, we speculate that NK-cell dysfunction is the primary reason *Eri1*$^{-/-}$ chimeras poorly controlled MCMV viral load. However, we cannot rule out the possibility that other hematopoietic populations may contribute to diminished viral clearance. Further study is required to fully define the extent of Eri1 regulation of immune responses.

Reduced NK-cell expansion was evident when equal numbers of WT and *Eri1*$^{-/-}$ Ly49H^{+} NK cells were transferred to Ly49H-deficient hosts, suggesting an NK cell–intrinsic defect. *Eri1*$^{-/-}$ NK cells also displayed a modest defect in IFN-γ production on cross-linking of ITAM-associated receptors in vitro, suggesting a general defect in activating receptor signal transduction that may contribute to poor viral control. Yet, on a per-cell basis, *Eri1*$^{-/-}$ and WT Ly49H^{+} NK cells surprisingly showed equal Ly49H-dependent degranulation and target cell killing. Thus, *Eri1*$^{-/-}$ NK cells are not generally hyporesponsive to Ly49H ligation or unable to mediate effector functions. In addition, reduced NK-cell expansion in MCMV infection does not reflect a general proliferation defect, as we observed normal IL-15–driven expansion in vitro and in vivo. Further research is needed to identify the affected pathways that mediate poor expansion of *Eri1*$^{-/-}$ Ly49H^{+} NK cells during MCMV infection.

Although we do not yet understand how Eri1 modulates mature miRNA abundance, we speculate that it acts by direct enzymatic

degradation of precursor or mature miRNAs, as is observed for the small RNA exonucleases SDN1 in *Arabidopsis* and XRN-2 in *C elegans*.[50,51] More generally, our data suggest that Eri1-dependent regulation of endogenous small RNAs in mammalian somatic cells is distinctly different from that observed in *S pombe* or *C elegans*, where Eri1 regulates endo-siRNA abundance. Deep sequencing analysis of small RNAs in WT and Eri1-deficient T cells revealed no small RNA species that were as dependent on Eri1 as some classes of endo-siRNAs are in *C elegans*. Thus, miRNAs are likely the major small RNA target for Eri1 in somatic mammalian cells. This activity may not be restricted to mammals, as one previous report found that *eri-1* mutant *C elegans* expressed increased levels of mature miR-238.[20]

We cannot exclude the possibility that other Eri1 substrates, such as ribosomal RNA, may mediate some of the phenotypes observed in *Eri1*$^{-/-}$ lymphocytes. Interestingly, *Eri1*$^{-/-}$ mice share some phenotypic similarities with humans who have Diamond-Blackfan anemia (DBA),[15] a heterogeneous disease most commonly attributed to *Rps19* mutations.[52] Lymphocyte deficiency is a common feature of many ribosomopathies including DBA, Shwachman-Diamond syndrome, and dyskeratosis congenita.[53] Of note, we were unable to detect NK-cell homeostasis defects in *Rps19* mutant mice (*Dsk3*) or *Rps20* mutants (*Dsk4*; data not shown).[54] Studies are currently under way to determine whether NK-cell deficiency occurs in other mouse strains with mutations in ribosome-associated proteins.

These results imply that miRNAs as a class are negatively regulated in lymphocytes and, by extension, so is miRNA-mediated gene silencing. Although Eri1 is broadly expressed because of its constitutive role in 5.8S rRNA maturation, it is enriched in lymphoid organs and is strongly up-regulated in activated lymphocytes. Thus, Eri1-mediated repression of miRNAs may lead to cell-type–specific defects. In this capacity, Eri1 comprises a growing class of factors that modulate miRNA expression at a global level.[14] Many of these factors, including Eri1, are attractive therapeutic targets whose inhibition could enhance miRNA- or siRNA-mediated gene repression.

Acknowledgments

The authors thank Ariya Lapan, Laura Smith, and Eric Yanni for technical assistance; Chris Eisley, Rebecca Barbeau, Andrea Barczak, and David Erle (SABRE Functional Genomics Core) for expert assistance with microarray experiments; Jon Woo (University of California, San Francisco [UCSF] Genomics Core Facility) for assistance with small RNA sequencing; Natalie Bezman for critical comments on the manuscript; and Joseph Sun, Sandra Lopez-Verges, Maelig Morvan, and Yosuke Kamimura for helpful discussions.

This work was supported by the Burroughs Wellcome Fund (CABS 1006173), the National Institutes of Health (NIH; HL109102 [K.M.A.], and AI089828, AI70788 and AI068129 [L.L.L.]), the German Research Foundation (DFG HE 3359/3-1), and the UCSF/NIH Medical Scientist Training Program (M.F.T.).

L.L.L. is an American Cancer Society Professor.

Authorship

Contribution: M.F.T. and K.M.A. performed research, analyzed data, and wrote the manuscript; S.A.-W. and M.P. performed some of the T-cell experiments, including miRNA qPCR for transduced T cells (S.A.-W.); J.E.B., M.R., and P.W. assisted with small RNA deep sequencing analysis and statistics; and K.M.A. and M.F.T. designed research with critical input from L.L.L. and V.H.

Conflict-of-interest disclosure: The authors declare no competing financial interests.

Correspondence: K. Mark Ansel, PhD, Department of Microbiology and Immunology, University of California San Francisco, 513 Parnassus Ave, Box 0414, San Francisco, CA 94143-0414; e-mail: mark.ansel@ucsf.edu.

References

1. Vivier E, Tomasello E, Baratin M, Walzer T, Ugolini S. Functions of natural killer cells. *Nat Immunol.* 2008;9(5):503-510.
2. Lanier LL. Up on the tightrope: natural killer cell activation and inhibition. *Nat Immunol.* 2008;9(5):495-502.
3. Arase H, Mocarski ES, Campbell AE, Hill AB, Lanier LL. Direct recognition of cytomegalovirus by activating and inhibitory NK cell receptors. *Science.* 2002;296(5571):1323-1326.
4. Smith HR, Heusel JW, Mehta IK, et al. Recognition of a virus-encoded ligand by a natural killer cell activation receptor. *Proc Natl Acad Sci U S A.* 2002;99(13):8826-8831.
5. Biron CA, Byron KS, Sullivan JL. Severe herpesvirus infections in an adolescent without natural killer cells. *N Engl J Med.* 1989;320(26):1731-1735.
6. Bukowski JF, Woda BA, Welsh RM. Pathogenesis of murine cytomegalovirus infection in natural killer cell-depleted mice. *J Virol.* 1984;52(1):119-128.
7. O'Connell RM, Rao DS, Chaudhuri AA, Baltimore D. Physiological and pathological roles for microRNAs in the immune system. *Nat Rev Immunol.* 2010;10(2):111-122.
8. Bezman NA, Cedars E, Steiner DF, Blelloch R, Hesslein DG, Lanier LL. Distinct requirements of microRNAs in NK cell activation, survival, and function. *J Immunol.* 2010;185(7):3835-3846.
9. Bezman NA, Chakraborty T, Bender T, Lanier LL. miR-150 regulates the development of NK and iNKT cells. *J Exp Med.* 2011;208(13):2717-2731.
10. Cichocki F, Felices M, McCullar V, et al. Cutting edge: microRNA-181 promotes human NK cell development by regulating Notch signaling. *J Immunol.* 2011;187(12):6171-6175.
11. Trotta R, Chen L, Ciarlariello D, et al. MiR-155 regulates IFN-gamma production in natural killer cells. *Blood.* 2012;119(15):3478-3485.
12. Baek D, Villen J, Shin C, Camargo FD, Gygi SP, Bartel DP. The impact of microRNAs on protein output. *Nature.* 2008;455(7209):64-71.
13. Selbach M, Schwanhausser B, Thierfelder N, Fang Z, Khanin R, Rajewsky N. Widespread changes in protein synthesis induced by microRNAs. *Nature.* 2008;455(7209):58-63.
14. Siomi H, Siomi MC. Posttranscriptional regulation of microRNA biogenesis in animals. *Mol Cell.* 2010;38(3):323-332.
15. Ansel KM, Pastor WA, Rath N, et al. Mouse Eri1 interacts with the ribosome and catalyzes 5.8S rRNA processing. *Nat Struct Mol Biol.* 2008;15(5):523-530.
16. Gabel HW, Ruvkun G. The exonuclease ERI-1 has a conserved dual role in 5.8S rRNA processing and RNAi. *Nat Struct Mol Biol.* 2008;15(5):531-533.
17. Bühler M, Verdel A, Moazed D. Tethering RITS to a nascent transcript initiates RNAi- and heterochromatin-dependent gene silencing. *Cell.* 2006;125(5):873-886.
18. Iida T, Kawaguchi R, Nakayama J. Conserved ribonuclease, Eri1, negatively regulates heterochromatin assembly in fission yeast. *Curr Biol.* 2006;16(14):1459-1464.
19. Duchaine TF, Wohlschlegel JA, Kennedy S, et al. Functional proteomics reveals the biochemical niche of C. elegans DCR-1 in multiple small-RNA-mediated pathways. *Cell.* 2006;124(2):343-354.
20. Lee RC, Hammell CM, Ambros V. Interacting endogenous and exogenous RNAi pathways in Caenorhabditis elegans. *RNA.* 2006;12:589-597.
21. Kennedy S, Wang D, Ruvkun G. A conserved siRNA-degrading RNase negatively regulates RNA interference in C. elegans. *Nature.* 2004;427(6975):645-649.
22. Bühler M, Mohn F, Stalder L, Mühlemann O. Transcriptional silencing of nonsense codon-containing immunoglobulin minigenes. *Mol Cell.* 2005;18(3):307-317.
23. Fodil-Cornu N, Lee SH, Belanger S, et al. Ly49h-deficient C57BL/6 mice: a new mouse cytomegalovirus-susceptible model remains resistant to unrelated pathogens controlled by the NK gene complex. *J Immunol.* 2008;181(9):6394-6405.
24. Orr MT, Sun JC, Hesslein DG, et al. Ly49H signaling through DAP10 is essential for optimal

natural killer cell responses to mouse cytomegalovirus infection. *J Exp Med.* 2009;206(4):807-817.

25. Arens R, Wang P, Sidney J, et al. Cutting edge: murine cytomegalovirus induces a polyfunctional CD4 T cell response. *J Immunol.* 2008;180(10):6472-6476.
26. Griffiths-Jones S, Saini HK, van Dongen S, Enright AJ. miRBase: tools for microRNA genomics. *Nucleic Acids Res.* 2008;36(Database issue):D154-D158.
27. Benjamini Y, Hochberg Y. Controlling the false discovery rate: a practical and powerful approach to multiple testing. *J Royal Stat Soc* 1995;57:289-300.
28. Thomas MF, Ansel KM. Construction of small RNA cDNA libraries for deep sequencing. *Methods Mol Biol.* 2010;667:93-111.
29. Babiarz JE, Ruby JG, Wang Y, Bartel DP, Blelloch R. Mouse ES cells express endogenous shRNAs, siRNAs, and other Microprocessor-independent, Dicer-dependent small RNAs. *Genes Dev.* 2008;22(20):2773-2785.
30. Steiner DF, Thomas MF, Hu JK, et al. MicroRNA-29 regulates T-box transcription factors and interferon-gamma production in helper T cells. *Immunity.* 2011;35(2):169-181.
31. Wu Z, Jenkins BD, Rynearson TA, et al. Empirical bayes analysis of sequencing-based transcriptional profiling without replicates. *BMC Bioinformatics.* 2010;11:564.
32. Kim S, Iizuka K, Kang HS, et al. In vivo developmental stages in murine natural killer cell maturation. *Nat Immunol.* 2002;3(6):523-528.
33. Ma A, Koka R, Burkett P. Diverse functions of IL-2, IL-15, and IL-7 in lymphoid homeostasis. *Annu Rev Immunol.* 2006;24:657-679.
34. Sun JC, Beilke JN, Lanier LL. Adaptive immune features of natural killer cells. *Nature.* 2009;457(7229):557-561.
35. Williams NS, Moore TA, Schatzle JD, et al. Generation of lytic natural killer 1.1+, Ly-49- cells from multipotential murine bone marrow progenitors in a stroma-free culture: definition of cytokine requirements and developmental intermediates. *J Exp Med.* 1997;186(9):1609-1614.
36. Williams NS, Klem J, Puzanov IJ, Sivakumar PV, Bennett M, Kumar V. Differentiation of NK1.1+, Ly49+ NK cells from flt3+ multipotent marrow progenitor cells. *J Immunol.* 1999;163(5):2648-2656.
37. Lee SH, Girard S, Macina D, et al. Susceptibility to mouse cytomegalovirus is associated with deletion of an activating natural killer cell receptor of the C-type lectin superfamily. *Nat Genet.* 2001;28(1):42-45.
38. Brown MG, Dokun AO, Heusel JW, et al. Vital involvement of a natural killer cell activation receptor in resistance to viral infection. *Science.* 2001;292(5518):934-937.
39. Orange JS, Biron CA. Characterization of early IL-12, IFN-alphabeta, and TNF effects on antiviral state and NK cell responses during murine cytomegalovirus infection. *J Immunol.* 1996;156(12):4746-4756.
40. Pien GC, Satoskar AR, Takeda K, Akira S, Biron CA. Cutting edge: selective IL-18 requirements for induction of compartmental IFN-gamma responses during viral infection. *J Immunol.* 2000;165(9):4787-4791.
41. Munks MW, Gold MC, Zajac AL, et al. Genome-wide analysis reveals a highly diverse CD8 T cell response to murine cytomegalovirus. *J Immunol.* 2006;176(6):3760-3766.
42. Loh J, Chu DT, O'Guin AK, Yokoyama WM, Virgin HW. Natural killer cells utilize both perforin and gamma interferon to regulate murine cytomegalovirus infection in the spleen and liver. *J Virol.* 2005;79(1):661-667.
43. Fehniger TA, Wylie T, Germino E, et al. Next-generation sequencing identifies the natural killer cell microRNA transcriptome. *Genome Res.* 2010;20(11):1590-1604.
44. Gent JI, Lamm AT, Pavelec DM, et al. Distinct phases of siRNA synthesis in an endogenous RNAi pathway in C. elegans soma. *Mol Cell.* 2010;37(5):679-689.
45. Guo H, Samarakoon A, Vanhaesebroeck B, Malarkannan S. The p110 delta of PI3K plays a critical role in NK cell terminal maturation and cytokine/chemokine generation. *J Exp Med.* 2008;205(10):2419-2435.
46. Tassi I, Presti R, Kim S, Yokoyama WM, Gilfillan S, Colonna M. Phospholipase C-gamma 2 is a critical signaling mediator for murine NK cell activating receptors. *J Immunol.* 2005;175(2):749-754.
47. Salcedo M, Diehl AD, Olsson-Alheim MY, et al. Altered expression of Ly49 inhibitory receptors on natural killer cells from MHC class I-deficient mice. *J Immunol.* 1997;158(7):3174-3180.
48. Bakker AB, Hoek RM, Cerwenka A, et al. DAP12-deficient mice fail to develop autoimmunity due to impaired antigen priming. *Immunity.* 2000;13(3):345-353.
49. Daniels KA, Devora G, Lai WC, O'Donnell CL, Bennett M, Welsh RM. Murine cytomegalovirus is regulated by a discrete subset of natural killer cells reactive with monoclonal antibody to Ly49H. *J Exp Med.* 2001;194(1):29-44.
50. Ramachandran V, Chen X. Degradation of microRNAs by a family of exoribonucleases in Arabidopsis. *Science.* 2008;321(5895):1490-1492.
51. Chatterjee S, Grosshans H. Active turnover modulates mature microRNA activity in Caenorhabditis elegans. *Nature.* 2009;461(7263):546-549.
52. Willig TN, Draptchinskaia N, Dianzani I, et al. Mutations in ribosomal protein S19 gene and diamond blackfan anemia: wide variations in phenotypic expression. *Blood.* 1999;94(12):4294-4306.
53. Khan S, Pereira J, Darbyshire PJ, et al. Do ribosomopathies explain some cases of common variable immunodeficiency? *Clin Exp Immunol.* 2010;163(1):96-103.
54. McGowan KA, Li JZ, Park CY, et al. Ribosomal mutations cause p53-mediated dark skin and pleiotropic effects. *Nat Genet.* 2008;40(8):963-970.